Environment Canada   Environnement Canada

Estimation of SO_2 and NO_2 emissions from point sources using satellite retrievals

Vitali Fioletov[1], Chris McLinden[1],

with contribution from

N. Krotkov[2], C. Li[2,3] , D. G. Loyola[4] , P. Valks[4], N. Theys[5], M. Van Roozendael[5], C. R. Nowlan[6], K. Chance[7], X. Liu[7], C. Lee[8], R. V. Martin[6,7]

[1]Environment Canada, Toronto, ON, Canada
[2]Atmospheric Chemistry and Dynamics Laboratory, NASA Goddard Space Flight Center, Greenbelt , MD USA
[3]Earth System Science Interdisciplinary Center, University of Maryland, College Park, MD USA
[4]Deutsches Zentrum für Luft- und Raumfahrt (DLR), Wessling, Germany
[5]Belgian Institute for Space Aeronomy (BIRA-IASB), Brussels, Belgium
[6]Department of Physics and Atmospheric Science, Dalhousie University, Halifax, Nova Scotia, Canada
[7]Harvard-Smithsonian Center for Astrophysics, Cambridge, MA, USA
[8]National Institute of Meteorological Research, Korea Meteorological Administration, Seoul, South Korea

Outline

- Satellite data analysis
- Emission estimates from satellite data
- Global SO_2 sources
- Applications for Canada, oil sands
- Validation of satellite data, Pandora spectrometer

Merging satellite data and meteorology

Mean SO_2 from OMI near Thompson, Manitoba (55N, 98 W).

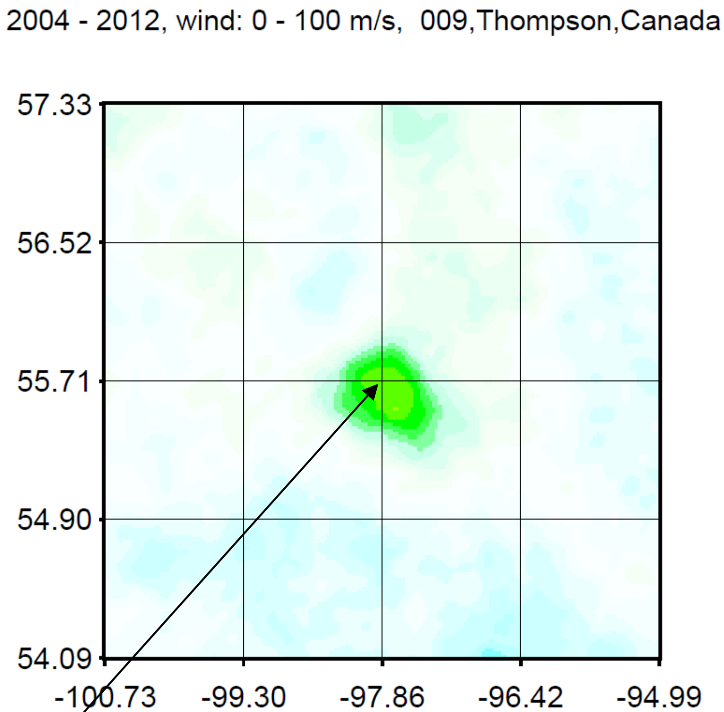

The same data after rotation of all pixels around the source in a upwind-downwind direction.

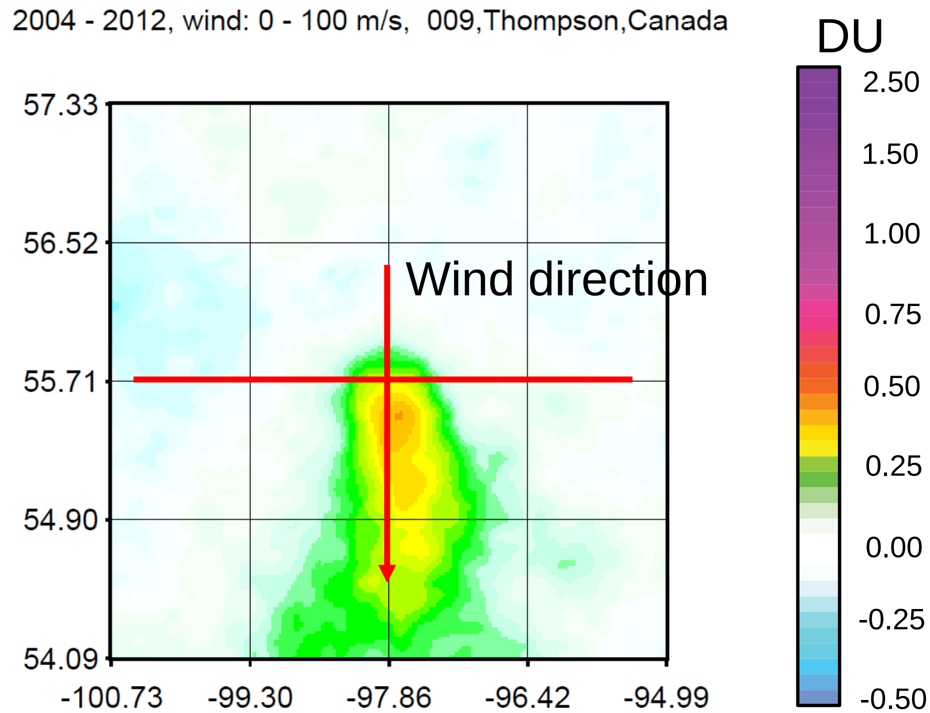

Downwind decay of pollutants can be studied using a rotation scheme in which the locations of all observation are adjusted so that the have a common wind-direction

Environment Canada   Environnement Canada

DALHOUSIE UNIVERSITY Inspiring Minds   Smithsonian   BIRA-IASB   DLR   NASA

The fitting algorithm: $OMI_{SO2} = a\, f(x,y)\, g(y,w)$

$f(x, y)$ - Gaussian function, $g(y, w)$ - Exponentially modified Gaussian function;

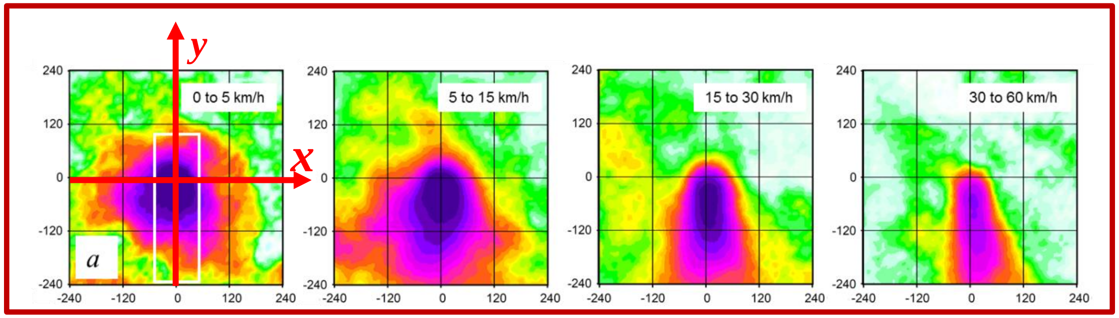

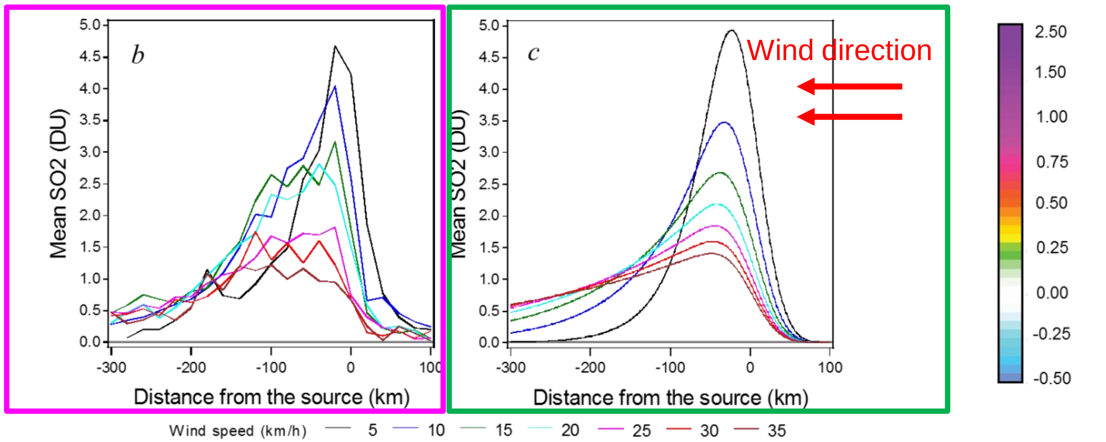

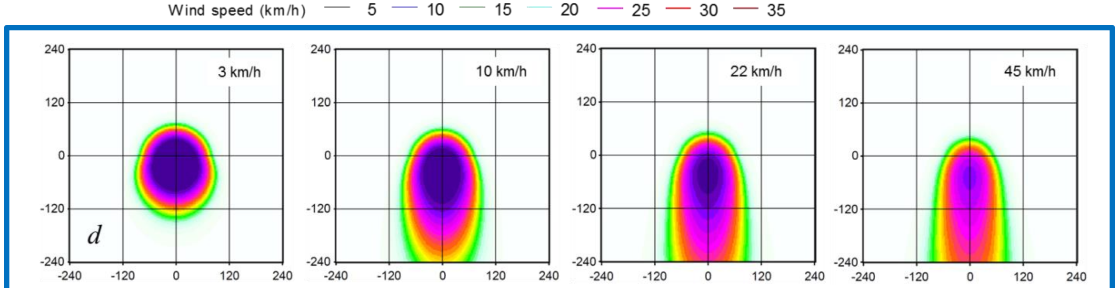

OMI PCA data:

a. Mean total column SO_2 (in DU) near **Norilsk (69°N, 88°E)** after rotation of all pixels in a upwind-downwind direction for 2005-2013 stratified by the wind speed. The axis show the distance from the source in km.

b. Mean total column SO_2 near Norilsk for different wind speed groups for the area within ±50 km across the wind direction (the white rectangle in (a)) as a function of the distance from the source (negative for the downwind), after rotation of all pixels in a upwind-downwind direction.

Fitting results:

c. Exponentially modified Gaussian function $g(y, w)$, where y is the distance from the source and w is the wind speed that represents the best fit to Norilsk data on the left.

d. The fitting results for different wind speeds as indicated on the plot.

Fioletov et al., submitted to GRL, 2014

Environment Canada Environnement Canada

DALHOUSIE UNIVERSITY *Inspiring Minds* · Smithsonian · BIRA-IASB · DLR · NASA

The fitting algorithm: $OMI_{SO2} = a\, f(x,y)\, g(y,w)$

$f(x, y)$ - Gaussian function, $g(y, w)$ - Exponentially modified Gaussian function;

x, y are the coordinates, w is the wind speed

It is assumed that SO_2 concentrations (emitted from a point source) decline with time (t) as $exp(-\lambda t)$, i.e., with a constant decay rate ($\tau = 1/\lambda$)

σ represents the spread due to diffusion

$$f(x,y) = \frac{1}{\sigma_1\sqrt{2\pi}} exp\left(-\frac{x^2}{2\sigma_1^2}\right);$$

$$g(y,w) = \frac{\lambda_1}{2} exp\left(\frac{\lambda_1(\lambda_1\sigma^2 + 2y)}{2}\right) \cdot erfc\left(\frac{\lambda_1\sigma^2 + y}{\sqrt{2}\sigma}\right);$$

$$\sigma_1 = \begin{cases} \sqrt{\sigma^2 - 1.5y}, y < 0 \\ \sigma, y \geq 0 \end{cases};$$

$$\lambda_1 = \lambda / w;$$

$$erfc(x) = \frac{2}{\sqrt{\pi}} \int_x^{\infty} e^{-t^2} dt$$

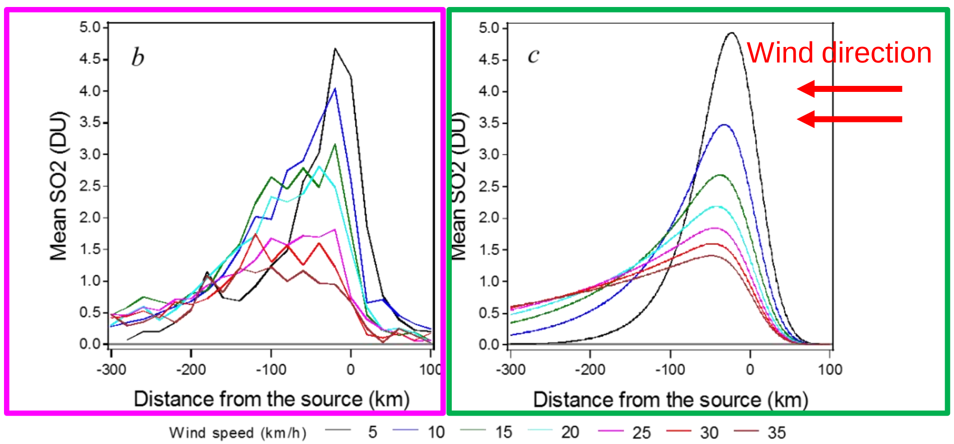

Parameters σ, λ, and a, were estimated from the fit

Since $\int_{-\infty}^{\infty}\int_{-\infty}^{\infty} f(x,y)\cdot g(y,w)dxdy = \int_{-\infty}^{\infty}(\int_{-\infty}^{\infty} f(x,y)dx)\cdot g(y,w)dy = \int_{-\infty}^{\infty} g(y,w)dy = 1$, a is the SO_2 mass

Emissions: $E = a/\tau$, where (1) τ is prescribed or (2) estimated as $1/\lambda$

Estimation of emissions from US major sources using OMI PCA data

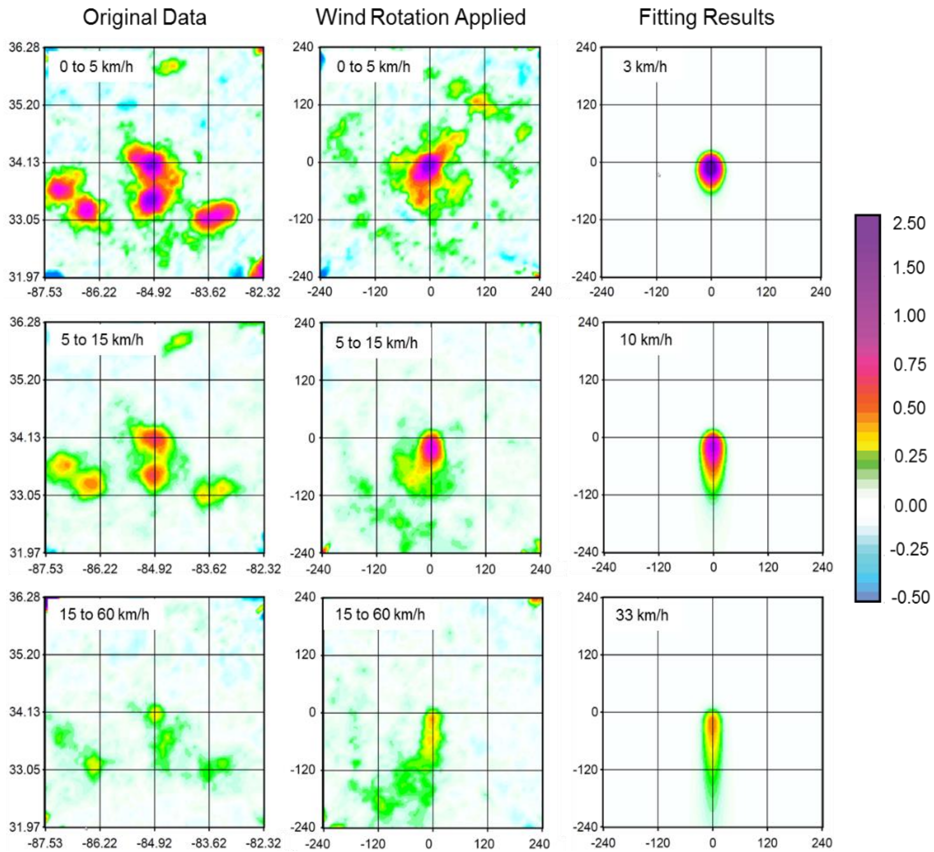

The mean column SO_2 values (in DU) for 2005-2007 near the largest US SO_2 source (**Bowen power plant in Georgia**, 170 kt y^{-1} in 2005) located in the center of each plot. The data are stratified by the wind speed. The right column demonstrates the fitting results for different wind speeds as indicated on the plot.

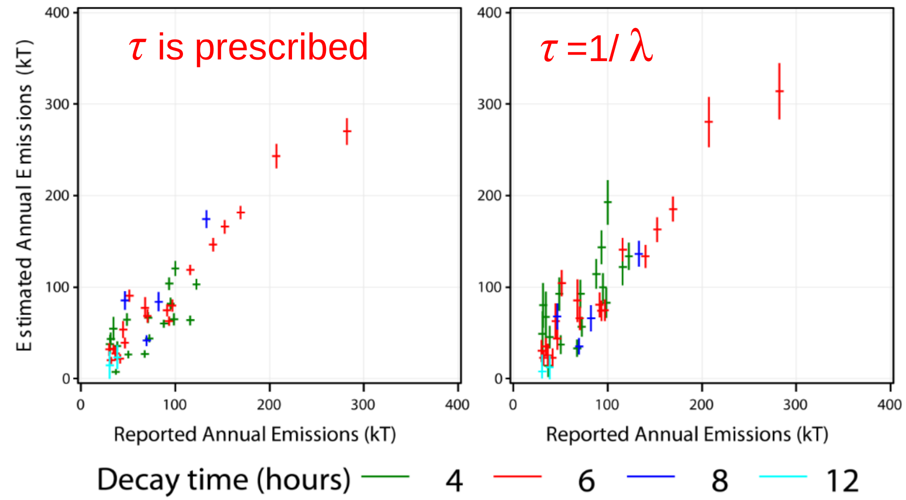

(left) Scatter plots of annual SO_2 emission from the largest US sources in 2005 vs. emissions calculated from OMI data for 2005-2007 assuming a constant the decay time (τ=6 hours) estimated from the best fit of the reported emissions

(right) The same plot but with emissions calculated from OMI data with both parameters estimated from the fit. Emissions are given in kt y^{-1} calculated assuming a constant emission rate.

The error bars represent the one sigma confidence intervals. Different colors indicate estimated decay times ($\tau = 1/\lambda$).

Fioletov et al., submitted to GRL, 2014

OMI SO_2 "catalogue"

- The detectability levels about 70 kt per year for the old OMI PBL data and ~30 kt per year for OMI PCA data
- >200 sources can be detected
- emissions to be derived, some not currently in inventories

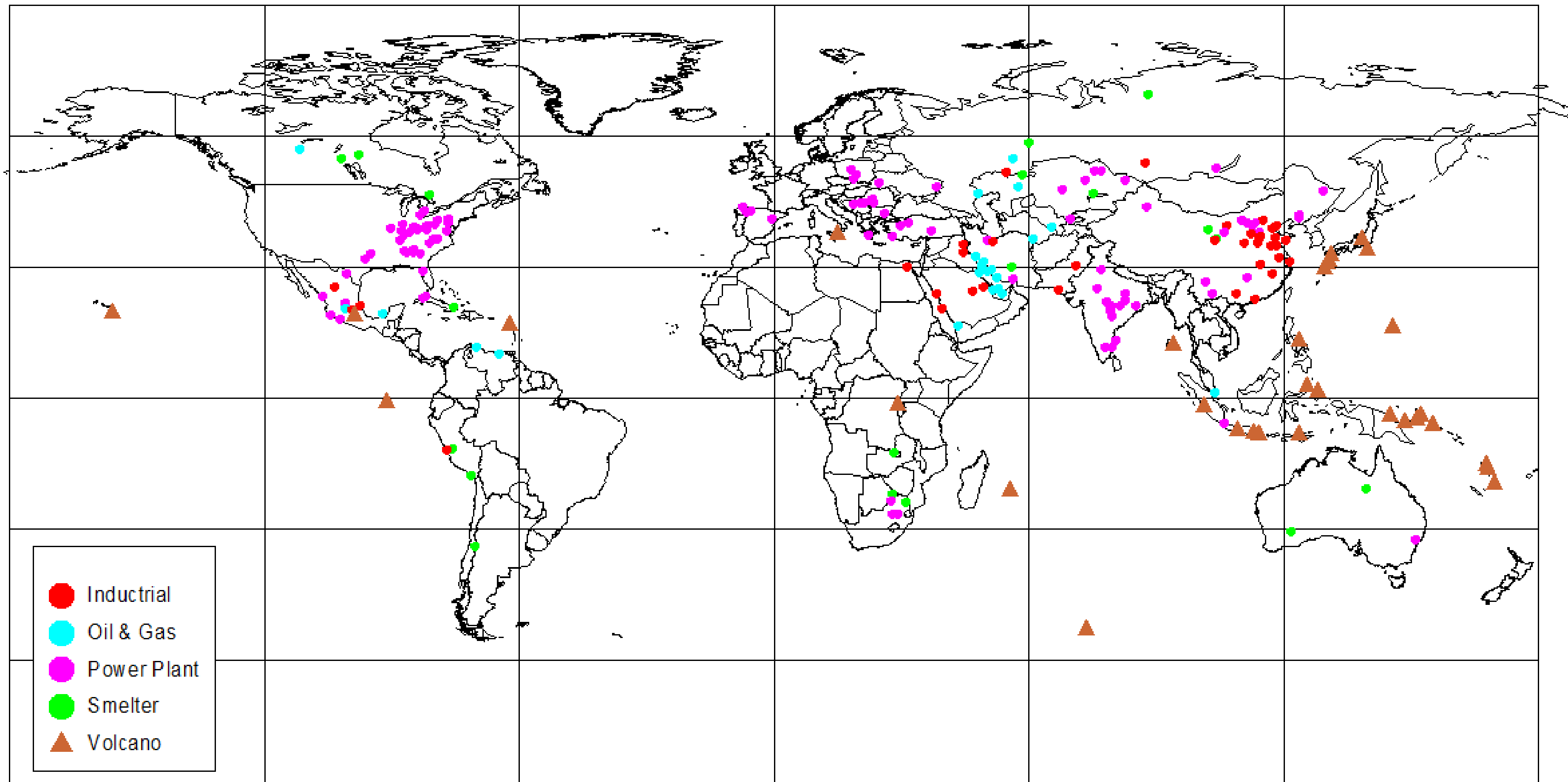

… still work in progress

SCIAMACHY and GOME 2 are less sensitive than OMI.

They can only see ~30 individual sources out of ~200 seen by OMI. Case study: Megalopolis, Greece, one of the largest SO2 emission sources in Europe (230 kT/y in 2007), in on the border of their sensitivity

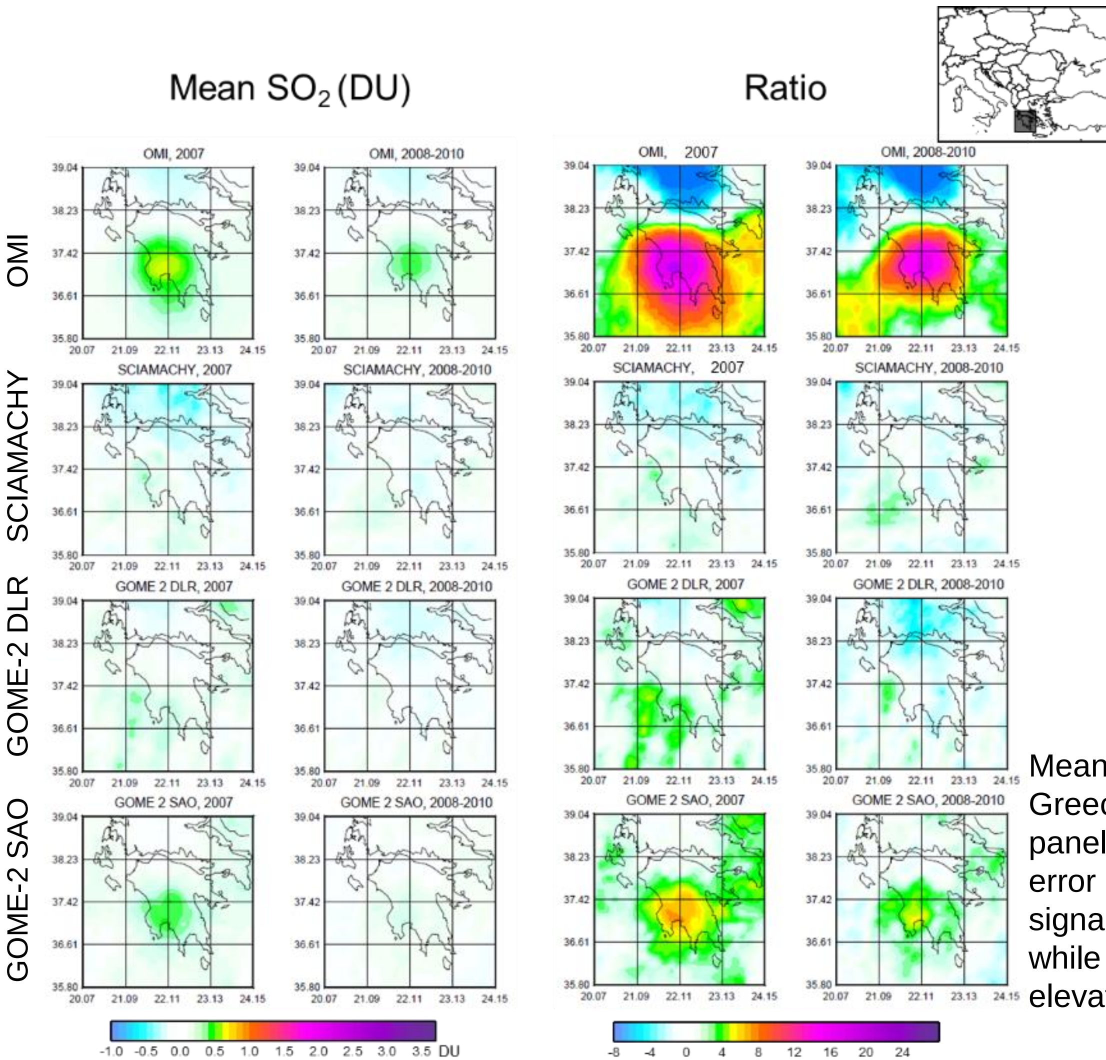

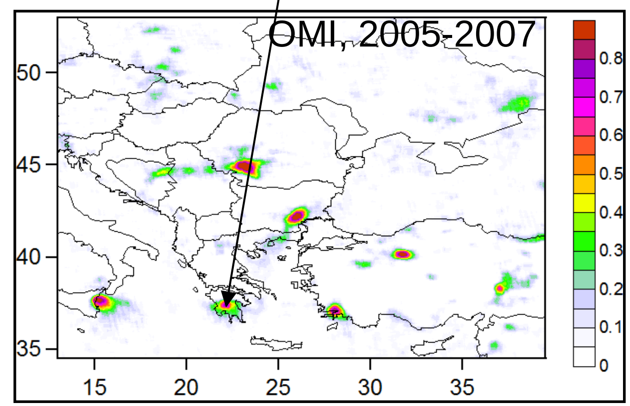

Mean SO_2 distribution over Megalopolis power plants, Greece, in DU. (left panel) SO_2 values in DU and (right panel) the rations between the mean SO_2 and the standard error of the mean are shown. No statistically significant signal appears in SCIAMACHY and GOME-2 DLR data, while OMI and GOME-2 SAO data show significantly elevated SO_2 values in the vicinity of the power plants.

Fioletov et al., JGR, 2013

OMI view of Central Canada

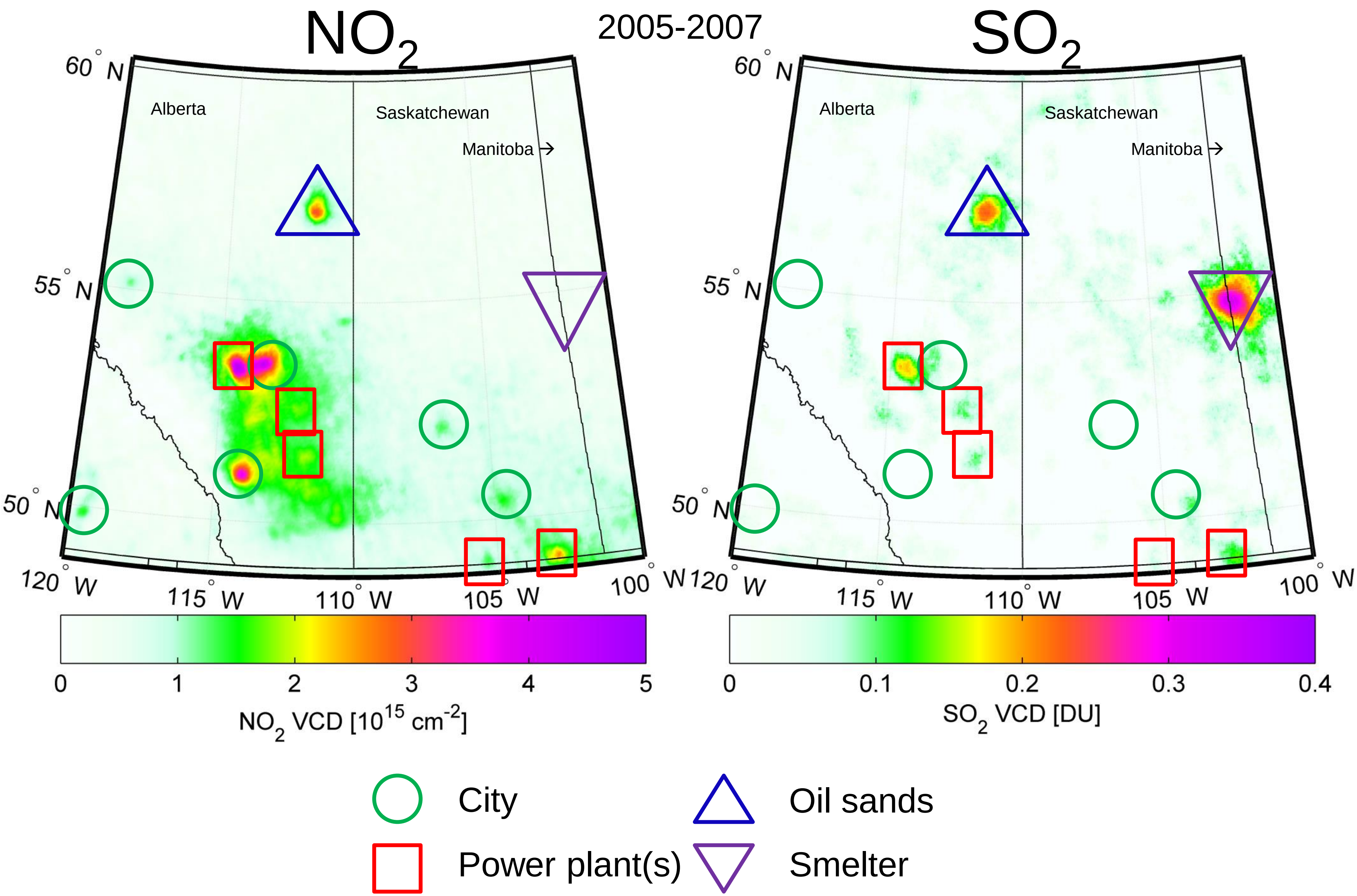

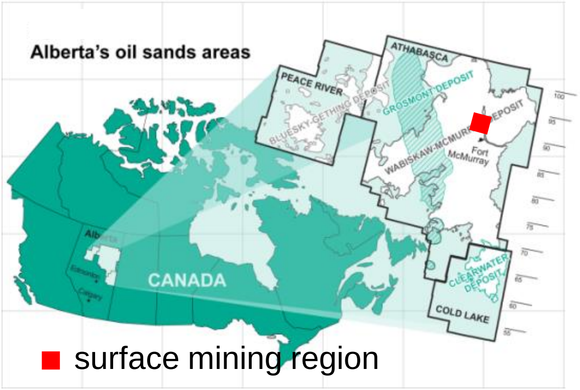

Oil sands monitoring

- Oil sands refers to a type of petroleum deposit in which the oil is very thick and sticky (called "bitumen") and mixed with sand, water, and clay
- Canada has a proven reserve of ~170 billion barrels with production increase from 0.7 mBPD (2000), 1.8 mBPD (2010), to 3.8 mBPD (2020)
- Surface mining & upgrading processes emit NO_x and SO_2 into the atmosphere

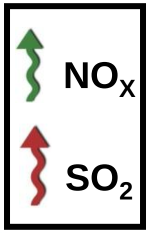

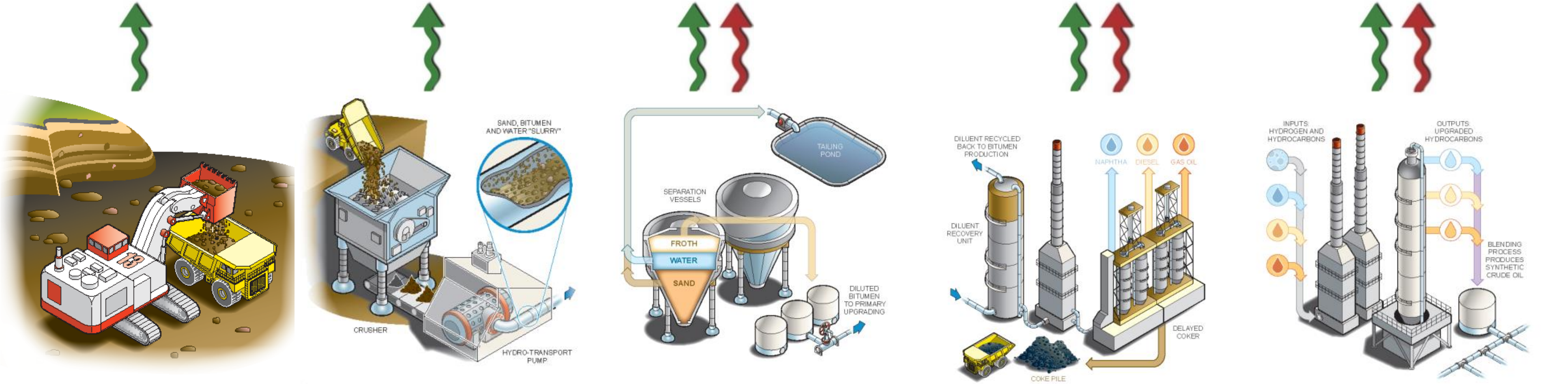

Mining & Transport | Extraction | Separation | Primary Upgrading | Secondary Upgrading

from The Oil Sands Process, CNRL

Steps in Surface Mining

Environment Canada   Environnement Canada

OMI SO_2 over the oil sands

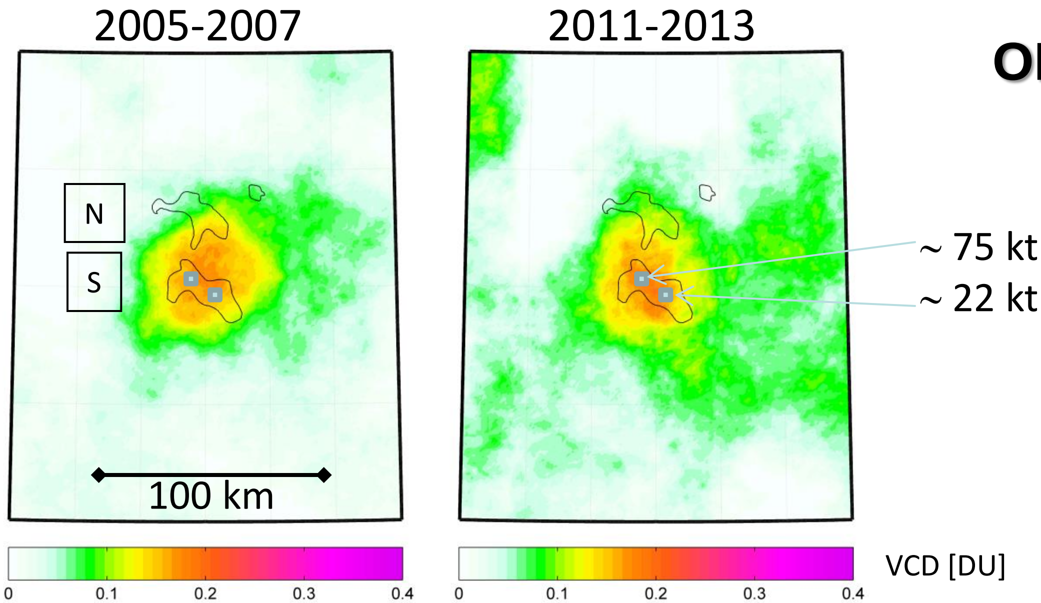

SO_2 emissions due to "upgrading" (converting bitumen to synthetic crude)

- Only two significant sources, both in southern, S ,mining region
- Northern mines pipe bitumen off-site for upgrading

2005 – 2013 average	E(NPRI*) = 100 kt[SO_2]/yr	E(OMI) = 89±19 kt[SO_2]/yr	τ = 4.3 hours
	*NPRI = National Pollutant Release Inventory		

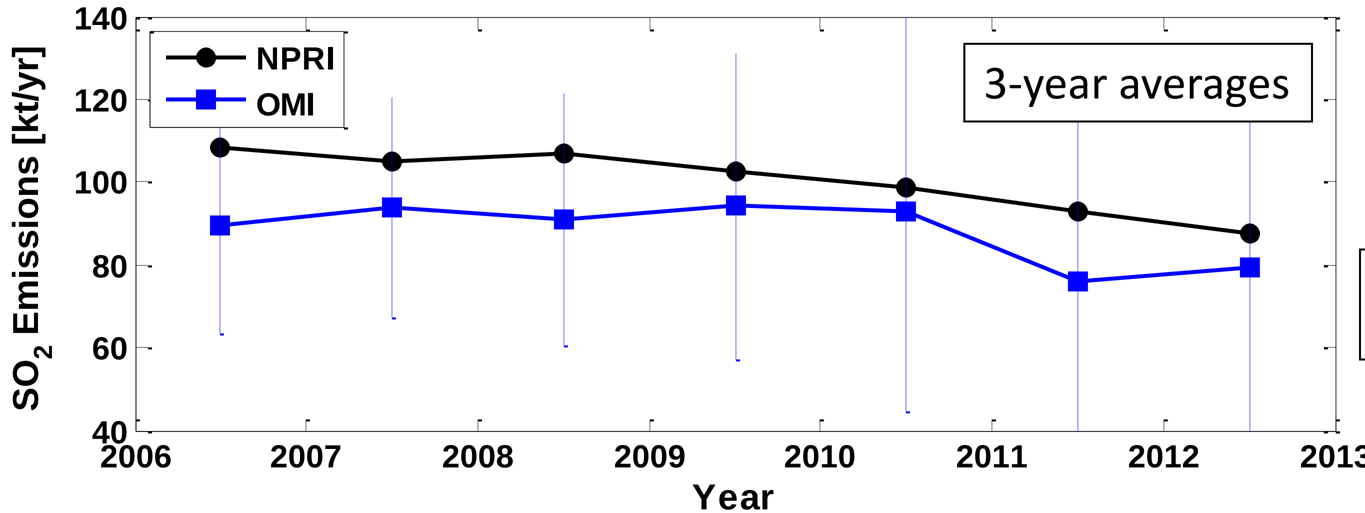

τ fixed at 4.3 hours to stabilize fits

Environment Canada Environnement Canada

OMI NO_2 over the oil sands

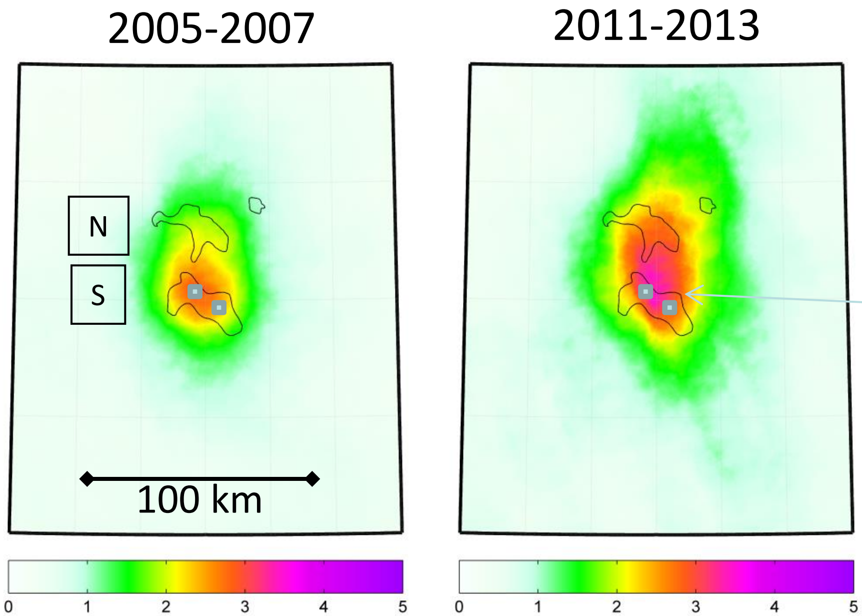

NO_2 emissions due to “upgrading” (~50%) (converting bitumen to synthetic crude) and large vehicles (~50%, more uncertain)

- Two significant point sources S (upgraders), both in southern mining region,
- Significant area sources in N and S
- Change in distribution consistent with expansion into the north

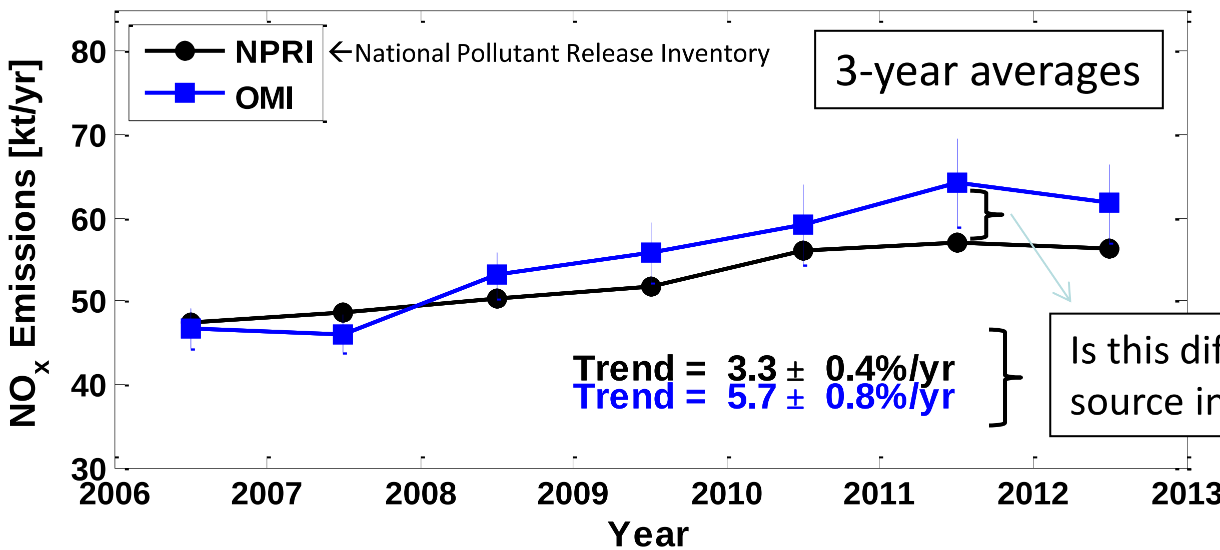

E and τ determined by fitting the downwind decay of NO_2 [similar to Beirle et al., Science, 2011]

$NOx / NO_2 = 1.35$ assumed

Is this difference real, from missing source in NPRI (e.g., construction) ?

Estimated NO_2 lifetime is about 2.5 hours

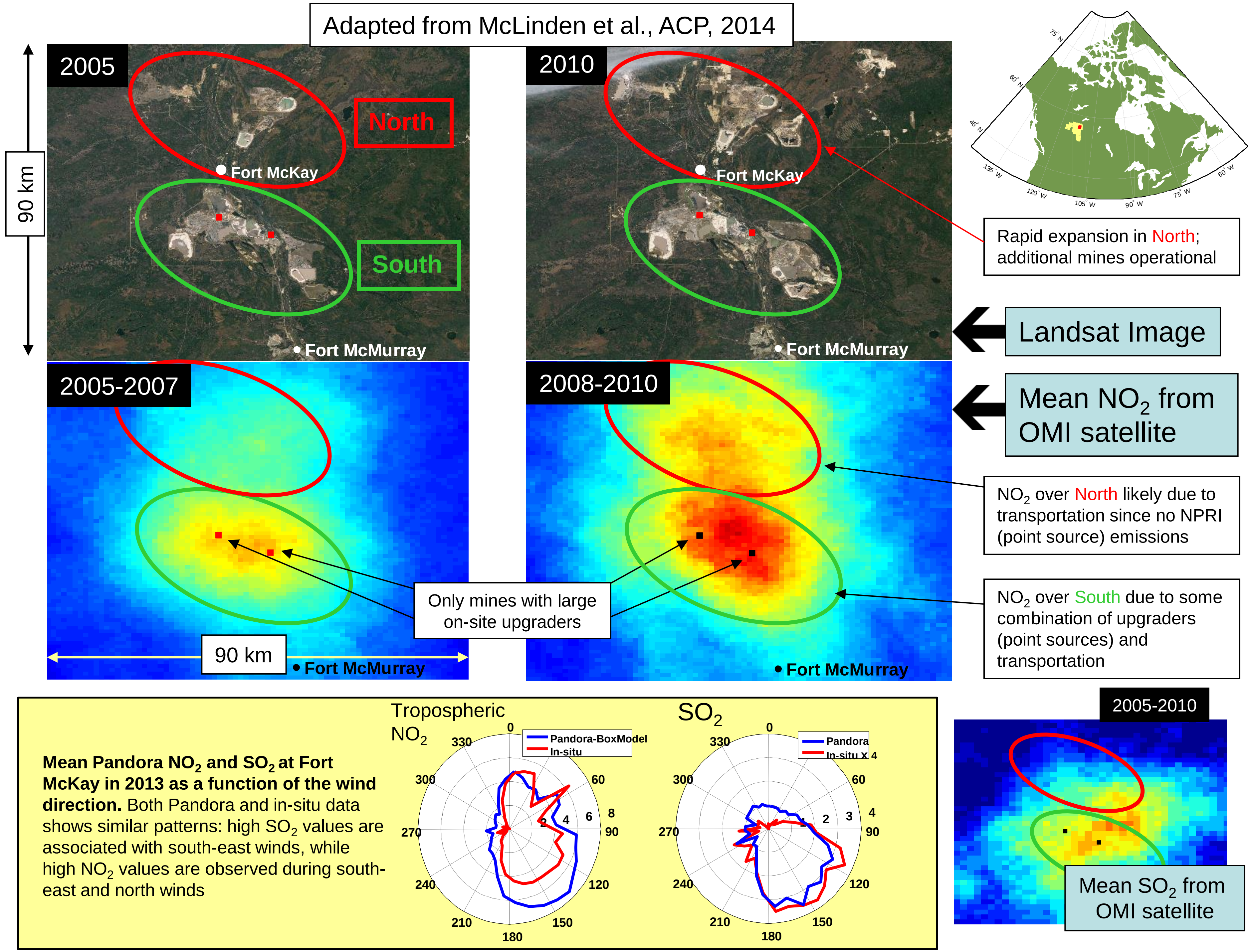

Adapted from McLinden et al., ACP, 2014
2005
2010
North
South
Fort McKay
Fort McMurray
90 km
Rapid expansion in North; additional mines operational
Landsat Image
2005-2007
2008-2010
Mean NO_2 from OMI satellite
NO_2 over North likely due to transportation since no NPRI (point source) emissions
NO_2 over South due to some combination of upgraders (point sources) and transportation
Only mines with large on-site upgraders
2005-2010
Mean SO_2 from OMI satellite
Tropospheric NO_2
Pandora-BoxModel
In-situ
SO_2
Pandora
In-situ x 4
Mean Pandora NO_2 and SO_2 at Fort McKay in 2013 as a function of the wind direction. Both Pandora and in-situ data shows similar patterns: high SO_2 values are associated with south-east winds, while high NO_2 values are observed during south-east and north winds

ement

Remote Sensing Instruments (CIMEL and Pandora), EC site at Fort McKay

Pollution episode at Fort McKay on August 23, 2013

Pandora spectrometer was installed at Fort McKay in August 2013. Pandora operates in DS DOAS mode using spectral range 300 nm-500 nm to retrieve Ozone, SO_2 and NO_2.

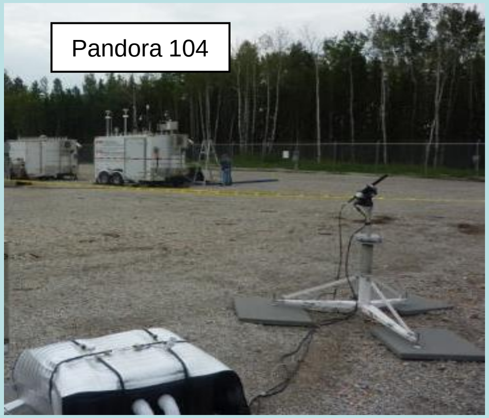

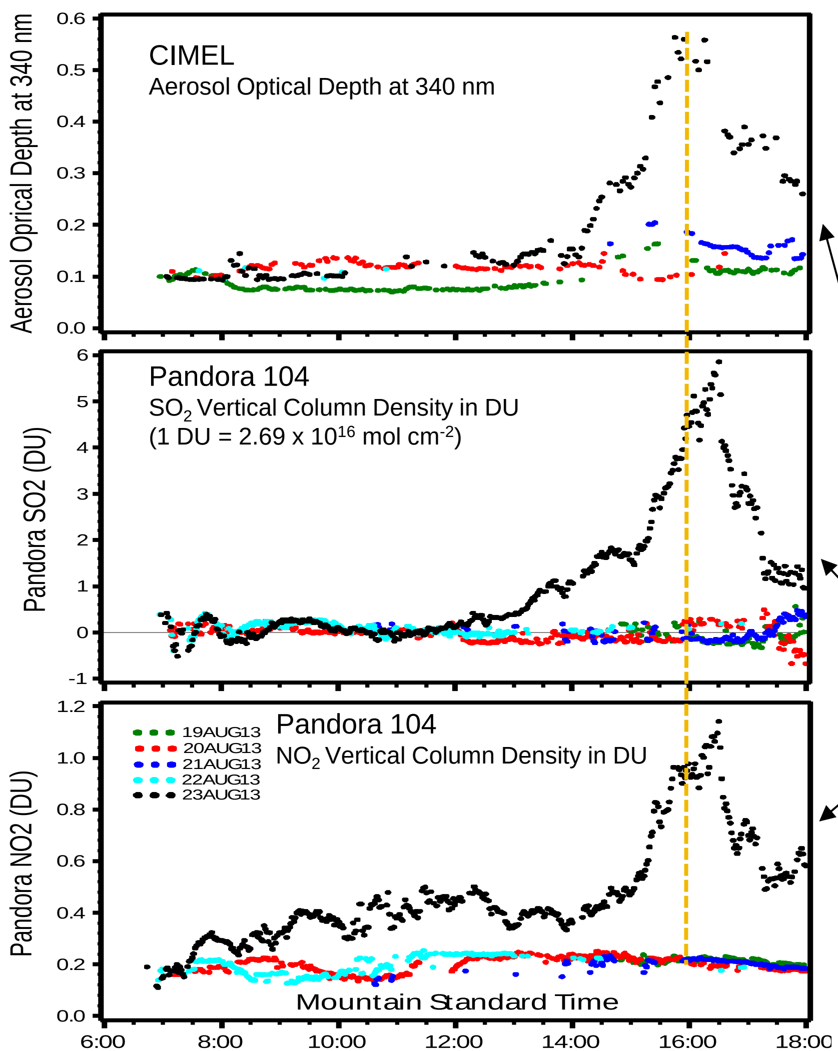

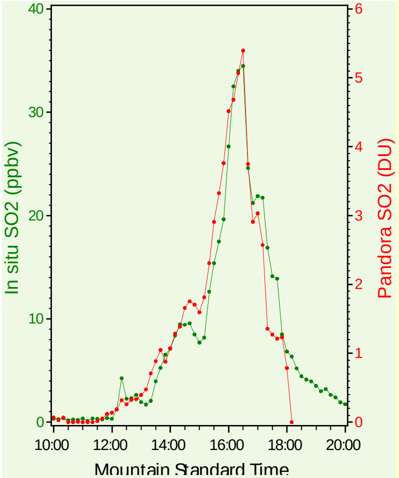

Pandora vs. in-situ

August 23 is in black

Different colours represent different days

Pandora-OMI NO_2 comparison

- New EC AMF based on 15 km x 15 km resolution AQ model (McLinden et al., ACP, 2014)
- EC AMF increases NO_2 and SO_2 over the mining area by factors of 2 and 1.4 respectively
- EC AMFs substantially improves agreement as compared to operational algorithms

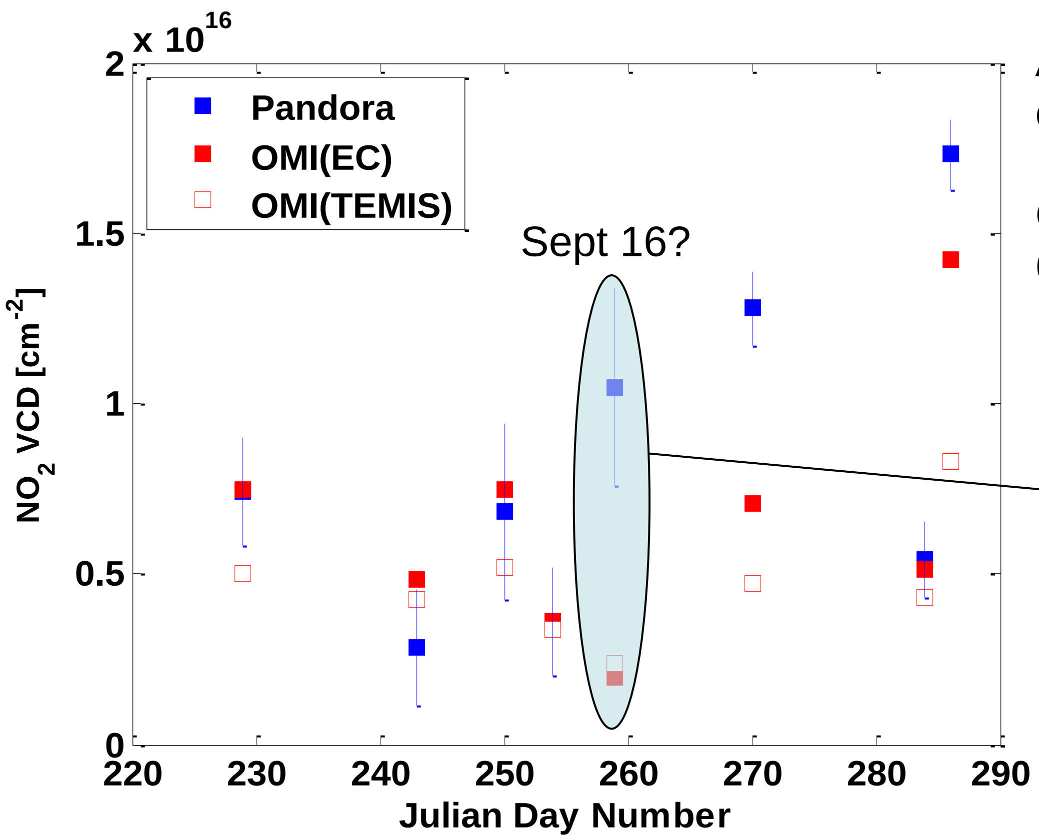

After filtering and cloud-screening, only 8 coincidences (in ~60 days)

Good quantitative consistency on 5 or 6 days

Pandora location

Environment Canada Environnement Canada

Possible Canadian ground-based remote-sensing sites for satellite validation

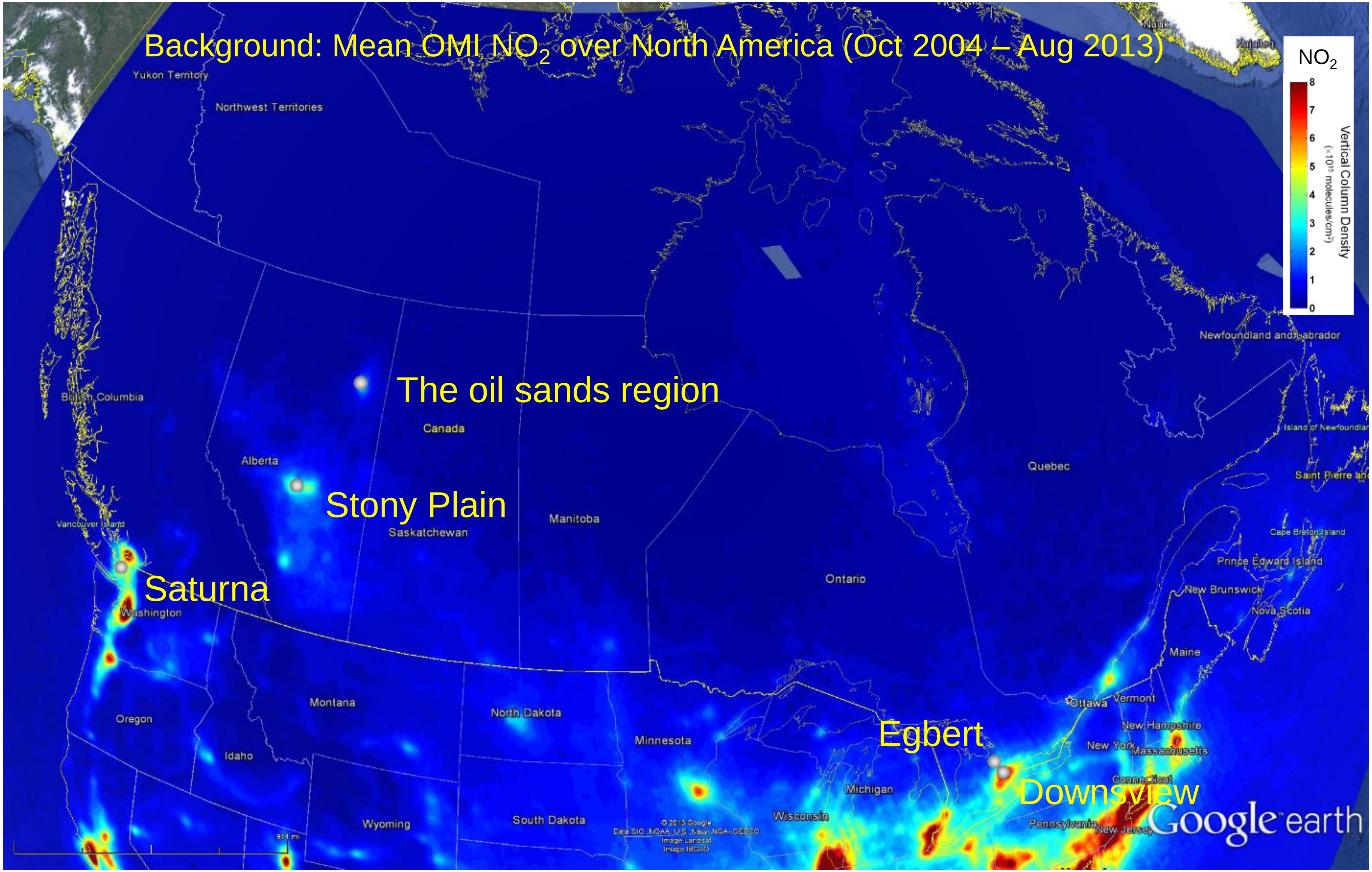

Environment Canada Environnement Canada

DALHOUSIE UNIVERSITY Inspiring Minds

Smithsonian

BIRA-IASB

DLR

NASA

Thanks for your attention!

Fioletov, V. E., C. A. McLinden, N. Krotkov, M. D. Moran, and K. Yang (2011), Estimation of SO_2 emissions using OMI retrievals, *Geophys. Res. Lett*., 38, L21811, doi:10.1029/2011GL049402.

McLinden, C.A., V. Fioletov, K. F. Boersma, N. Krotkov, C. E. Sioris, J. P. Veefkind, and K. Yang, Air quality over the Canadian oil sands: A first assessment using satellite observations, *Geophys. Res. Lett*., 39, 4, doi:10.1029/2011GL050273, 2012

Fioletov, V. E., C. A. McLinden, N. Krotkov, K. Yang, D. G. Loyola, P. Valks, N. Theys, M. Van Roozendael, C. R. Nowlan, K. Chance, X. Liu, C. Lee, and R. V. Martin, Application of OMI, SCIAMACHY, and GOME-2 satellite SO_2 retrievals for detection of large emission sources, *J. Geophys. Res.*, 118, doi:10.1002/jgrd.50826, 2013.

McLinden, C. A., Fioletov, V., Boersma, K. F., Kharol, S. K., Krotkov, N., Lamsal, L., Makar, P. A., Martin, R. V., Veefkind, J. P., and Yang, K.: Improved satellite retrievals of NO2 and SO2 over the Canadian oil sands and comparisons with surface measurements, *Atmos. Chem. Phys.,* 13, 21609-21664, doi:10.5194/acpd-13-21609-2013, 2014.

Fioletov V.E, C. A. McLinden, N. Krotkov, and C. Li**,** Lifetimes and emissions of SO_2 from point sources estimated from OMI, *submitted to GRL*, 2014